

Experimental demonstration of four-channel WDM 560 Gbit/s 128QAM-DMT using IM/DD for 2-km optical interconnect

Citation for published version (APA):

Li, F., Yu, J., Cao, Z., Zhang, J., Chen, M., & Li, X. (2017). Experimental demonstration of four-channel WDM 560 Gbit/s 128QAM-DMT using IM/DD for 2-km optical interconnect. *Journal of Lightwave Technology*, 35(4), 941-948. [7723897]. <https://doi.org/10.1109/JLT.2016.2621052>

Document license:
TAVERNE

DOI:
[10.1109/JLT.2016.2621052](https://doi.org/10.1109/JLT.2016.2621052)

Document status and date:
Published: 15/02/2017

Document Version:
Publisher's PDF, also known as Version of Record (includes final page, issue and volume numbers)

Please check the document version of this publication:

- A submitted manuscript is the version of the article upon submission and before peer-review. There can be important differences between the submitted version and the official published version of record. People interested in the research are advised to contact the author for the final version of the publication, or visit the DOI to the publisher's website.
- The final author version and the galley proof are versions of the publication after peer review.
- The final published version features the final layout of the paper including the volume, issue and page numbers.

[Link to publication](#)

General rights

Copyright and moral rights for the publications made accessible in the public portal are retained by the authors and/or other copyright owners and it is a condition of accessing publications that users recognise and abide by the legal requirements associated with these rights.

- Users may download and print one copy of any publication from the public portal for the purpose of private study or research.
- You may not further distribute the material or use it for any profit-making activity or commercial gain
- You may freely distribute the URL identifying the publication in the public portal.

If the publication is distributed under the terms of Article 25fa of the Dutch Copyright Act, indicated by the "Taverne" license above, please follow below link for the End User Agreement:

www.tue.nl/taverne

Take down policy

If you believe that this document breaches copyright please contact us at:

openaccess@tue.nl

providing details and we will investigate your claim.

Experimental Demonstration of Four-Channel WDM 560 Gbit/s 128QAM-DMT Using IM/DD for 2-km Optical Interconnect

Fan Li, Jianjun Yu, Zizheng Cao, Junwen Zhang, Ming Chen, and Xinying Li

(Top-scored)

Abstract—In this paper, we experimentally demonstrated a four-channel wavelength-division-multiplex (WDM) 560 Gbit/s 128 quadrature amplitude modulation (128QAM)-Discrete MultiTone (DMT) signal transmission in a short reach interconnect. Coordinated discrete Fourier transform-spread and preequalization are jointly used to simultaneously overcome serious frequency domain power attenuation and reduce the peak-to-average power ratio of the DMT signal. An additional postdecision-directed least mean square equalizer is used afterward to further compensate the channel response and mitigate the devices' implementation penalty. These proposed algorithms and equalizer are validated through experiment in this paper, we achieved the highest capacity signal transmission in the four-channel WDM transmission system using intensity modulation and direct detection over a 2.4-km single mode fiber with a bit-error-ratio under the hard-decision forward error correction limit of 3.8×10^{-3} .

Index Terms—Decision-directed least mean square (DD-LMS), Discrete multitone (DMT), discrete Fourier transform-spread (DFT-spread), optical interconnect, preequalization, wavelength-division-multiplex (WDM).

I. INTRODUCTION

HIGH-DEFINITION video and high-speed broadband penetration and consumer IP traffic are responsible for the majority of the traffic growth, the optical communication system capacity demand has experienced explosive growth in the past decade. In the short reach optical communication systems, with the popularization of data centers and other bandwidth hungry interconnect applications, the desired

capacity of short reach networks has exponentially increased to 400 Gbit/s or even higher. 400-gigabit Ethernet (400 GbE) is now being discussed and standardized by IEEE task force 802.3 group [1]. Traditional electrical interconnect over coaxial cable solution cannot satisfy 400 Gbit/s signal transmission, optical interconnect becomes a good candidate for ultra-high speed signal transmission with lower cost and power consumption. Up to 2-km SMF 400 Gbit/s optical interconnect proposed for connection between transport networks and core routers as well as in the inter-connection of data centers has been widely discussed, low-cost solutions with intensity modulation and direction detection (IM/DD) is a good candidate for optical interconnect due to their low cost [1]–[15]. Transmission of 4λ 100 Gbit/s wavelength-division-multiplex (WDM) signal scheme is a cost-effective and low power consumption way to upgrade system capacity from 100 GbE to 400 Gbit/s class or beyond [4]–[10]. To satisfy high speed signal transmission in short reach optical fiber systems, several solutions with different advanced modulation formats, such as pulse amplitude modulation (PAM) [4], [5], [13], Discrete Multi-Tone (DMT) [6]–[8], [11]–[21] and carrier-less amplitude phase modulation (CAP) [9], [10], [13], have been proposed and demonstrated. DMT is a multi-carrier scheme which derives from orthogonal frequency division multiplexing (OFDM) with only a real valued signal. It inherits all advantages of OFDM signal, such as transparency to modulation formats and robustness to chromatic dispersion (CD) and polarization mode dispersion [18]–[21]. Among these four types of advanced modulation formats, DMT is the most practical as it is transparent to sub-carrier modulation formats and easy to upgrade system capacity with high-level modulation formats. Four O-band optical carriers 500 Gbit/s PAM4 signal transmission with direct detection is realized in [4]. However, the bandwidth requirement of the link in that work is relatively high (25 GHz) since the spectrum efficiency is limited by the PAM4 modulation format.

In order to reduce system devices' bandwidth requirements, realization of four-channel 560 Gbit/s 128 quadrature amplitude modulation (128QAM)-DMT signal transmission with direct detection is reported in our previous work [22]. This paper presents the extended work based on [22] with additional details and discussion, and also we introduce post decision-directed least mean square (DD-LMS) equalizer to further compensate

Manuscript received May 31, 2016; revised August 26, 2016 and October 5, 2016; accepted October 18, 2016. Date of publication October 26, 2016; date of current version February 22, 2017. This work is partly supported by the National Natural Science Foundation of China under Grants 61325002 and 61601199.

F. Li was with the ZTE (TX) Inc., Morristown, NJ 07960 USA. He is now with the Sun-Yat Sen University, Guangzhou 510275, China (e-mail: fanli0809@gmail.com).

J. Yu, X. Li, and J. Zhang are with the ZTE (TX) Inc., Morristown, NJ 07960 USA, and also with the Key Laboratory for Information Science of Electromagnetic Waves (MoE), Fudan University, Shanghai 200433, China (e-mail: jianjun@fudan.edu.cn; smileseaxy@gmail.com; hustzjw@gmail.com).

Z. Cao is with the Eindhoven University of Technology, Eindhoven 5612 AZ, The Netherlands (e-mail: z.cao@tue.nl).

M. Chen is with the ZTE (TX) Inc., Morristown, NJ 07960 USA (e-mail: ming.chen@hunu.edu.cn).

Color versions of one or more of the figures in this paper are available online at <http://ieeexplore.ieee.org>.

Digital Object Identifier 10.1109/JLT.2016.2621052

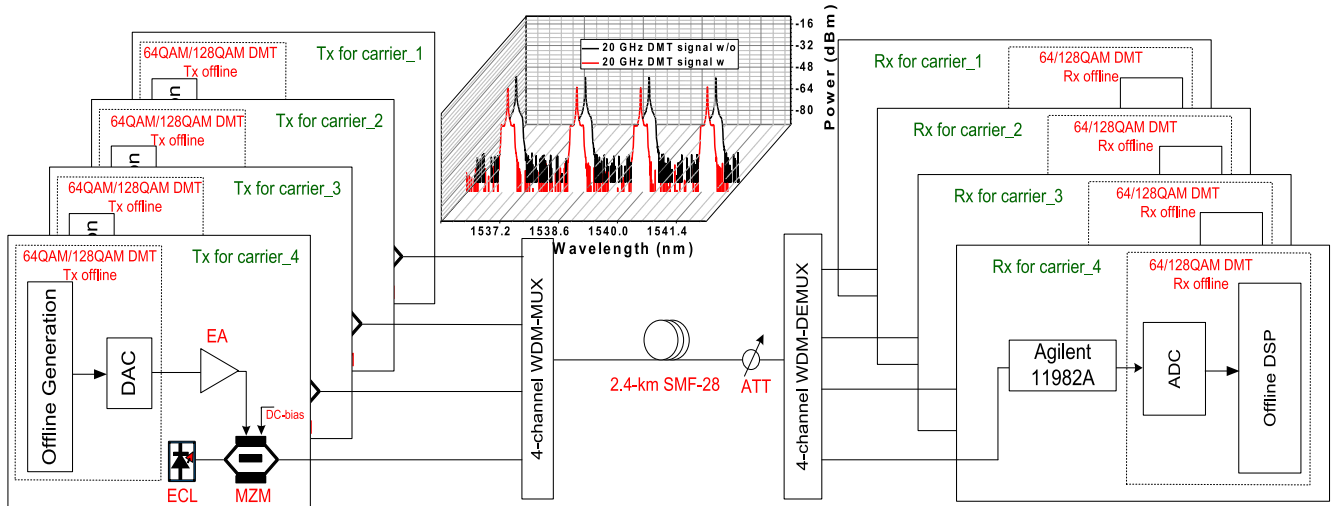


Fig. 1 Experimental system setup for 560 Gbit/s short reach system. DAC: digital to analog converter, EA: electrical amplifier, ECL: external cavity laser, MZM: Mach-Zehnder modulator, ATT: attenuator, ADC: analog to digital converter, Tx: transmitter, Rx: receiver, DSP: digital signal processing.

the channel response and mitigate the devices' implementation penalty [23], [24]. In Section II, we introduce the experimental setup for four channel 560 Gbit/s 128QAM-DMT signal transmission in detail. In Section III, we discuss the application of coordinated discrete Fourier Transform-spread (DFT-spread) and pre-equalization to simultaneously overcome frequency domain power attenuation and reduce the peak-to-average power ratio (PAPR) of the DMT signal. In Section IV, we discuss the realization of post DD-LMS equalizer to further compensate the channel response and mitigate the devices' implementation penalty in detail. In Section V, we present the experimental results of four WDM channel 560 Gbit/s 128QAM-DMT signal for both optical back-to-back (OBTB) and after 2.4-km SMF-28 transmission. In Section VI, we make the conclusion.

In this paper, after excluding all overheads which include training sequence (TS), cyclic prefix (CP) and 7% hard decision-forward error correction (HD-FEC) coding, the net data rate is 513.9 Gbit/s. As high spectrum efficiency 128QAM modulation format is used in the link, we only use 10 GHz class (15 GHz optical bandwidth and 11 GHz electrical bandwidth) receiver for 20 GHz 128QAM-DMT reception. We achieved a record capacity four-channel WDM signal transmission with direct-detection over 2.4-km SMF-28 with the bit error ratio (BER) under the HD-FEC limit of 3.8×10^{-3} based on 10 GHz class devices.

II. EXPERIMENTAL SETUP

Figure 1 shows the real-time experimental setup of the four-channel WDM 560 Gbit/s DMT transmission system with IM/DD. A summary of key parameters in the experimental setup is shown in Table 1. In the transmitter, there are four external cavity lasers (ECLs) at 1538.19, 1539.77, 1541.35 and 1542.94 nm with less than 100 kHz linewidth used as four WDM optical carriers. Four optical carriers are independently modulated by four different electrical baseband DMT signals with four 30 GHz 3-dB bandwidth Mach-Zehnder modulators (MZMs) with 20-dB extinction ratio. Four independent DMT signals are generated from 8-bit resolution Fujitsu digital-to-

TABLE I
KEY PARAMETERS IN THE EXPERIMENTAL SETUP

Parameters	Value
Wavelength of ECLs	1538.19/1539.77/1541.35/1542.94 nm
3-dB Bandwidth of MZMs	> 30 GHz
3-dB Bandwidth of EAs	25 GHz
Linewidth of ECLs	< 100 kHz
3-dB Bandwidth of Receivers	optical 15 GHz/electrical 11 GHz
Fiber Length	2.4 km
Sampling rate of DAC/ADC	80/80 GSa/s
Resolution of DAC/ADC	8/8 bits
FFT size of DMT signal	8192
Bandwidth of DMT signal	20 GHz
Modulation formats	64QAM/128QAM
Output Power of MZMs	7.8 dBm
Insertion Loss of coarse WDM coupler	< 1 dB

analog convertors (DACs) with 80 GSa/s maximum sampling rate and 16 GHz 3 dB bandwidth and then four cascaded linear electrical amplifiers (EAs) with 25 GHz 3-dB bandwidth are applied to boost the signal to 2.4 V to drive the MZMs. In this paper, 64QAM/128QAM DMT signal are tested in the transmission system. During the generation of 64QAM/128QAM-DMT signal, FFT size is 8192. Of the 8192 sub-carriers, 2048 are used to carry 64QAM/128QAM data, the total bandwidth of the generated DMT signal is 20 GHz when the DAC sampling rate is set at 80 GSa/s. In this paper, large FFT size is chosen to improve the frequency resolution during channel estimation to ensure good BER performance of the DMT signal transmission even with high-level modulation formats [16]. A 16-sample CP is added in the front of every 8192 samples, giving 8208 samples per one DMT symbol. In order to suppress the PAPR of DMT signal and overcome insufficient bandwidth caused inter-symbol interference (ISI) to some extent [20], the DFT-spread technique is implemented for the 2048 data carrying sub-carriers. According to numerical calculation, 3.4-dB PAPR improvement is attained at the probability of 2×10^{-4} with the DFT-spread technique. From the Table I we can see the bandwidth of the receiver in the experimental

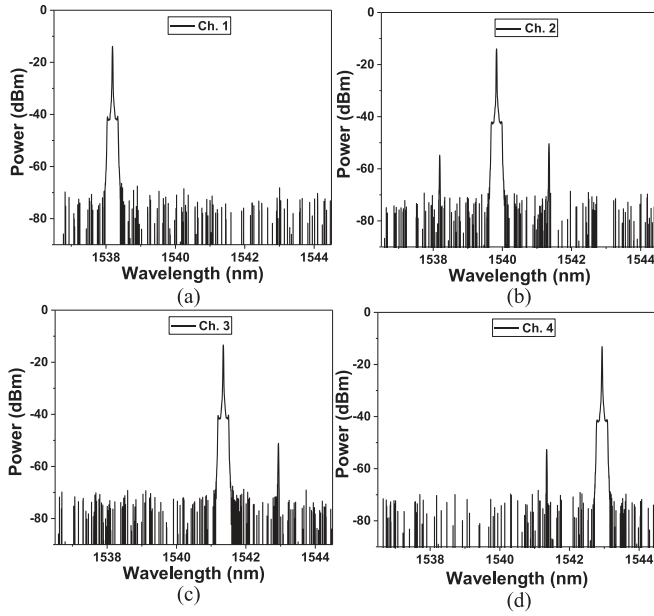


Fig. 2. Optical spectra of four branches (0.02-nm resolution).

setup is insufficient, and the DFT-spread technique mention in [20] is not good at resisting serious ISI. Taking this factor into consideration, frequency domain pre-equalization is applied to compensate serious high frequency attenuation to eliminate ISI [25]. In the experimental setup, the pre-equalization coefficients are obtained in the system calibration stage. There are 6/7 bits are mapped onto each 64QAM/128QAM symbol, the raw bit rate on each optical carrier is 120/140 Gbit/s for 64QAM/128QAM-DMT signal and the total bit rate of four optical carrier WDM system with 64QAM-DMT and 128QAM-DMT modulation formats are 480 Gbit/s and 540 Gbit/s, respectively. One TS symbol is added in the front of 60 DMT symbols for time synchronization and channel estimation. During optical DMT modulation, four commercial MZMs are all biased at the quadrature point of MZM power transmission curve with 7.8-dBm average output power separately. Four modulated optical carriers are combined by a 1×4 WDM-multiplexer (MUX) with 200 GHz channel spacing. The optical spectra (0.02-nm resolution) of combined four-channel WDM DMT signal with and without pre-equalization are shown in inset of Fig. 1. High frequency compensation can be clearly observed in the spectra. The fiber length in this experiment is only 2.4 km, thus an optical amplifier is not necessary in experimental setup. As the fiber length is quite short, no fiber nonlinear effects are observed in the transmission system.

After 2.4-km SMF-28 transmission, at the receiver, the received optical signal is first coupled into a 200-GHz grid WDM-demultiplexer (DEMUX), which is applied to filter out four optical carriers into four branches. The total loss of 2.4-km SMF-28 link is 0.8 dB. The insertion loss of the WDM-MUX and WDM-DEMUX are 0.8 and 1 dB, respectively. The optical spectra (0.02-nm resolution) of four branches are shown in Fig. 2. An optical attenuator before the 1×4 WDM-DEMUX is applied in the system to adjust the received optical power

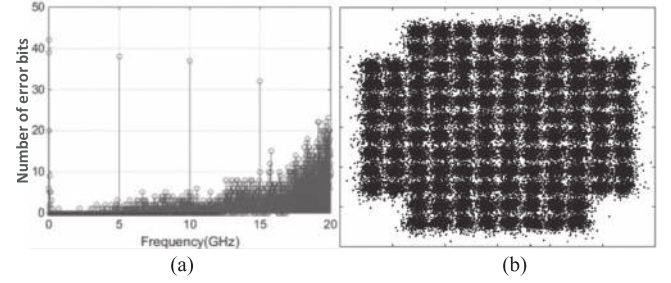


Fig. 3. (a) Error distribution and (b) constellation of traditional 20 GHz 128QAM-DMT in OBTB.

(ROP) into receivers in each branch. Four optical receivers (Agilent 11982A) with 15 GHz optical and 11 GHz electrical 3 dB bandwidth are used to realize optical to electrical conversion (O/E) for the optical DMT signal at the receiver. Four-channel converted electrical DMT signals are fed into four 8-bit ADCs operated at 80 GSa/s sampling rate with 3-dB bandwidth of 32 GHz. Finally, four ADC outputs are captured by a laptop and fed into off-line digital signal processing (DSP) for DMT demodulation. The off-line DSP includes resampling, time synchronization, removing CP, 8192-point FFT, frequency domain channel estimation and equalization, 2048-point IFFT for DFT-spread, DD-LMS equalizer to further compensate the channel response and mitigate the devices' implementation penalty, de-mapping and error counting. In this paper, BER was obtained by simple direct error counting with 120 DMT symbols ($120 \times 2048 \times 7 = 1720320$ bits).

III. COORDINATED DFT-SPREAD AND PRE-EQUALIZATION FOR DMT SIGNAL

In order to obtain comprehensive evaluation of system channel response, the number of error bits versus frequency is measured with 20-GHz traditional 128QAM-DMT signal in OBTB and the result is shown in Fig. 3(a). We find that much more error bits appear at some discrete frequency bins, such as 5, 10, 15 and 20 GHz, and frequency bins around zero frequency. The constellation of received 20 GHz 128QAM-DMT signal is shown in Fig. 3(b), it also shows that the overall BER performance of the signal should be very poor. As the signal is detected by a square-law photodiode in direct detection, sub-carrier to sub-carrier beating interference (SSBI) will lead to obvious BER performance degradation in low frequency [18]. Regarding the high BER at some discrete frequency bins, we believe that clock leakage in the DACs leads to signal noise ratio (SNR) degradation at these discrete frequency bins, thus the BER performance of these tones should be very poor. To achieve better BER performance, 6 low-frequency sub-carriers and sub-carriers at 5, 10, 15 and 20 GHz are not filled with data symbols in the DMT modulation. However, the number of total data carrying symbols is still maintained at 2048, while this will make the bandwidth boundary of DMT signal a little larger than 20 GHz.

DFT-spread is proposed for application in the transceiver side DSP to suppress the PAPR of the DMT signal and overcome high frequency power attenuation [16], [20], while DFT-spread

cannot cope well with bandwidth limitation induced serious ISI. In the experiment, the 3-dB bandwidth of some important transceiver devices, especially DACs and photodiodes, are insufficient for 20-GHz DMT signal transmission. As 64QAM or 128QAM modulation formats symbols are carried on each sub-carrier, other solutions except DFT-spread should be applied to resist serious ISI. Pre-equalization is an effective way to solve devices bandwidth limitation induced serious ISI, while PAPR of a DMT signal becomes even higher after pre-equalization. Taking these factors into consideration, we propose to use coordinated DFT-spread and pre-equalization to simultaneously suppress the PAPR of the DMT signal and overcome device bandwidth limitation induced serious ISI.

In the DMT signal transmission enabled with coordinated DFT-spread and pre-equalization, training sequences (TSs) for channel response acquisition can be generated with/without additional IFFT/FFT for DFT-spread. Without additional IFFT/FFT for DFT-spread, the samples in the TSs for transceiver's response estimation are discrete vector symbols, while the samples in the TSs with additional IFFT/FFT for DFT-spread are analog-like samples [21]. From this point of view, TSs without additional IFFT/FFT for DFT-spread should show better performance in acquiring accurate transceiver's response. During the pre-equalization procedure, accurate knowledge of the channel response should be obtained in the calibration stage in OBTB. Time domain repeated averaging method based channel estimation with TSs is used to obtain reliable transceiver's response. In the repeated averaging method, all the transmitted traditional DMT symbols without additional IFFT/FFT can be used as TSs in the transmitter. The total number of transmitted TSs in the repeated averaging method is 61 and the modulation format for all sub-carriers is QPSK. During estimation, TSs are first transmitted to estimate the transceiver's response and then these obtained channel response samples are averaged to suppress the random noise. As the transmission link attenuations are fully compensated in our pre-equalization scheme, pre-equalization coefficients can be simply obtained from the inversion of estimated channel response. The obtained pre-equalization coefficients are given in Fig. 4(a). It can be seen that the maximum power difference is larger than 12 dB, so serious power attenuation cannot be overcome by the DFT-spread algorithm only. The pre-equalization process is implemented for data carrying sub-carriers in frequency domain with obtained pre-equalization coefficients. Electrical spectra of 20 GHz DFT-spread 128QAM-DMT without and with pre-equalization are shown in Fig. 4(b) and 4(c), respectively. High frequency power attentions have been totally compensated after pre-equalization. The electrical spectrum of 20 GHz DFT-spread 128QAM-DMT with pre-equalization after 2.4 km SMF-28 is shown in Fig. 4(d), no CD induced power attenuation is observed for 20-GHz DMT signal after such a short length SMF transmission.

To verify the effectiveness of the coordinated DFT-spread and pre-equalization technique for DMT signal transmission, four types of 20 GHz 128QAM-DMT signal, traditional 128QAM-DMT, DFT-spread 128QAM-DMT, 128QAM-DMT with pre-equalization and DFT-spread 128QAM-DMT with pre-equalization are transmitted in OBTB. Distributions of the num-

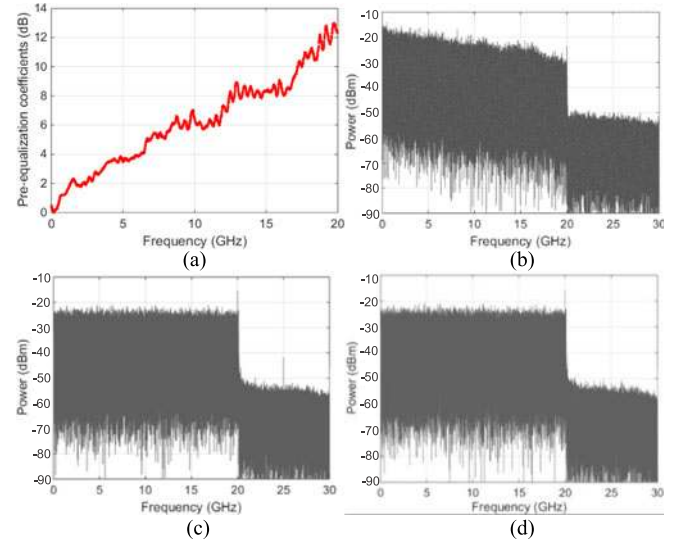


Fig. 4. (a) Pre-equalization coefficients, electrical spectra of 20 GHz (b) DFT-spread 128QAM-DMT in OBTB, (c) DFT-spread 128QAM-DMT with pre-equalization in OBTB and (d) DFT-spread 128QAM-DMT with pre-equalization after 2.4 km SMF.

ber of bits in error and constellations of four types of DMT signal given in Fig. 5. In Fig. 5(a), we can see that these error peaks mentioned above disappear, while the BER performance at high frequency is very poor. Compared to other three types of 128QAM-DMT signal, 128QAM-DMT signal with coordinated DFT-spread and pre-equalization demonstrated the best BER performance which is shown in Fig. 5(d), and its constellation in Fig. 5(h) is the most concentrated.

IV. DD-LMS EQUALIZER FOR DFT-SPREAD DMT SIGNAL

After frequency domain equalization and additional FFT for DFT-spread, direct decision boundaries of the constellation become clear, this will guarantee DD-LMS equalizer's stable-state operation. DD-LMS equalizer can be applied before final decision to further compensate the channel response and mitigate the devices' implementation penalty. The settings of the DD-LMS equalizer are controlled by:

$$J_{DD-LMS} = E \left\{ |d(k) - y(k)|^2 \right\} \quad (1)$$

of which $d(k)$ is the expected output and $y(k)$ is equalizer output. DD-LMS is a stochastic gradient descent algorithm, and does not depend on the statistics of symbols but relies on the symbol decisions. DD-LMS equalizer parameters' optimization can be realized according to steepest descent algorithm over Eq. (1). It can be realized with following rules:

$$y(k) = \mathbf{w}^H(k) \mathbf{X}(k) \quad (2)$$

$$e(k) = d(k) - y(k) \quad (3)$$

$$\mathbf{w}(k+1) = \mathbf{w}(k) + \mu e(k) \mathbf{X}^*(k) \quad (4)$$

where $\mathbf{X}(k) = [x(k) \ x(k-1) \ x(k-1) \ x(k-2) \ \dots \ x(k-N+1)]^T$ and $\mathbf{w}(k) = [w_0(k) \ w_1(k) \ w_2(k) \ w_3(k) \ \dots \ w_{N-1}(k)]^T$ represent input signal vectors and equalizer weight

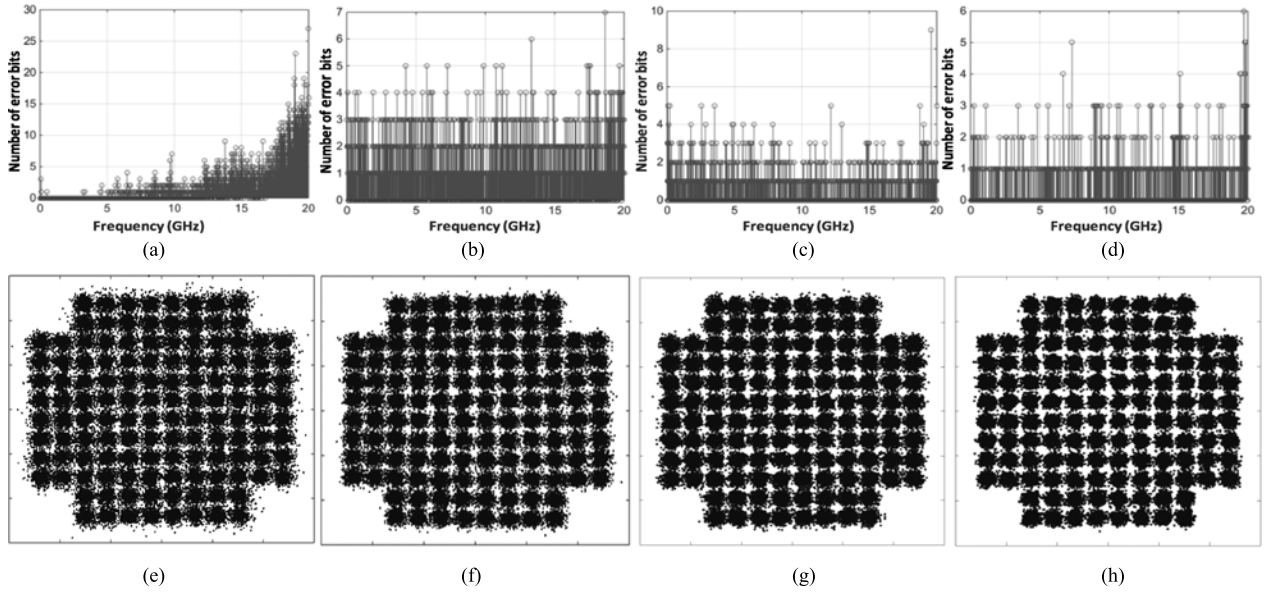


Fig. 5. Error distribution of (a) traditional 128QAM-DMT, (b) DFT-spread 128QAM-DMT, (c) 128QAM-DMT with pre-equalization, (d) DFT-spread 128QAM-DMT with pre-equalization and constellation of (e) traditional 128QAM-DMT, (f) DFT-spread 128QAM-DMT, (g) 128QAM-DMT with pre-equalization, (h) DFT-spread 128QAM-DMT with pre-equalization.

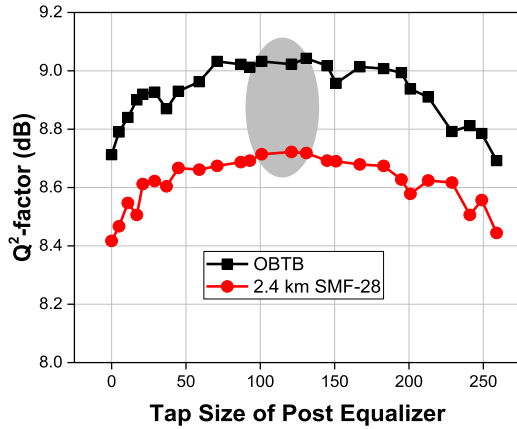


Fig. 6. Measured Q^2 -factor versus tap sizes of the post DD-LMS equalizer for 20-GHz DFT-spread 128QAM-DMT with pre-equalization.

vectors, respectively. N is the tap size of post equalizer. $()^H$ and $()^T$ denote the Hermitian and transposed matrix of $()$. $e(k)$ and μ are decision error signal and adaptation step size of the post equalizer.

To optimize the adaptation step size of T -spaced post DD-LMS equalizer, Q^2 -factor versus tap sizes of the post DD-LMS equalizer in OBTB and after 2.4 km SMF-28 for 20-GHz DFT-spread 128QAM-DMT with pre-equalization are measured and the results are shown in Fig. 6. In this paper, Q^2 -factor can be obtained according to standard relation between Q^2 -factor and BER [26]:

$$Q^2 = 20 \log_{10}(\sqrt{2} \text{erfcinv}(2\text{BER})) \quad (5)$$

With the tap size optimized in OBTB and after 2.4 km SMF-28 transmission, Q^2 -factor can be improved 0.3 dB and the

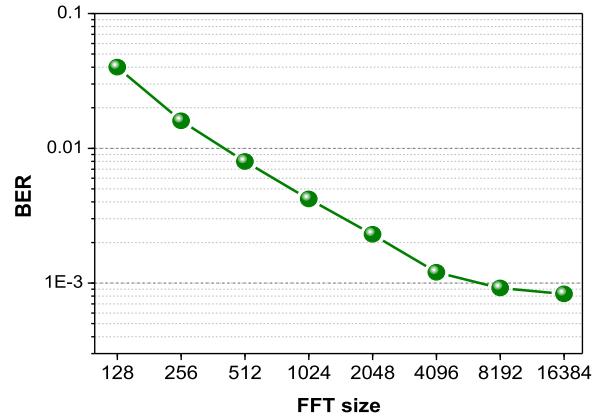


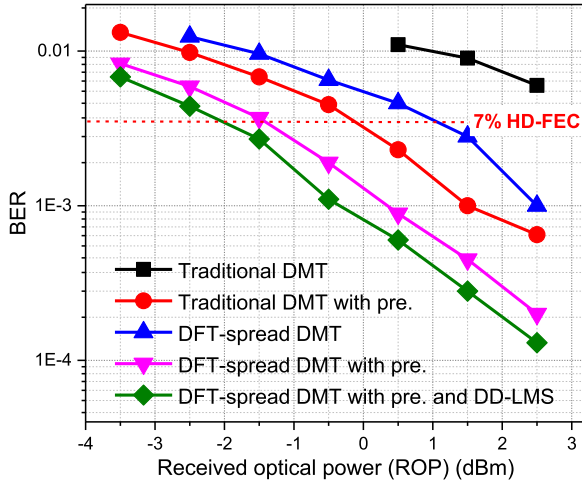
Fig. 7. Measured BER versus FFT size of 128QAM-DMT signal in OBTB.

transmission penalty is around 0.3 dB. Investigation shows that optimal tap size is from 101 to 127 for both cases.

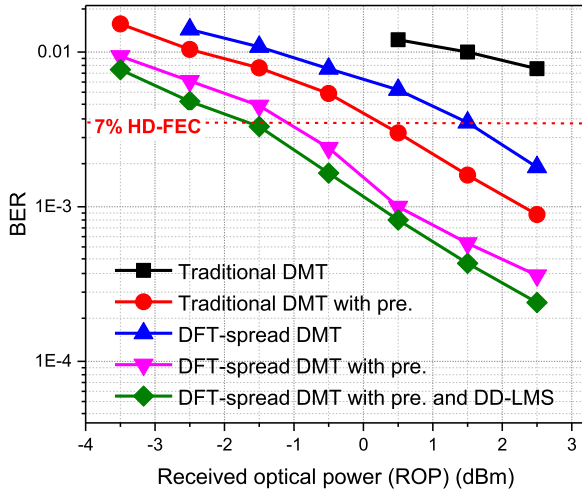
V. RESULTS AND DISCUSSIONS

The BER of 20 GHz DFT-spread 128QAM-DMT with pre-equalization and DD-LMS equalizer versus different FFT sizes is measured in OBTB and shown in Fig. 7. It can be seen that the BER performance is improved when the FFT size in the DMT modulation is increased. Taking spectrum efficiency, performance and computational complexity into consideration, 8192 FFT size is chosen in this paper.

In this paper, both 20 GHz 64QAM-DMT and 128QAM-DMT signals are tested in the experimental system. The BER of four types of 20 GHz 64QAM-DMT signals mentioned in Section III in the OBTB case and after 2.4-km SMF-28 transmission for the 2nd channel at 1539.77 nm are tested and the



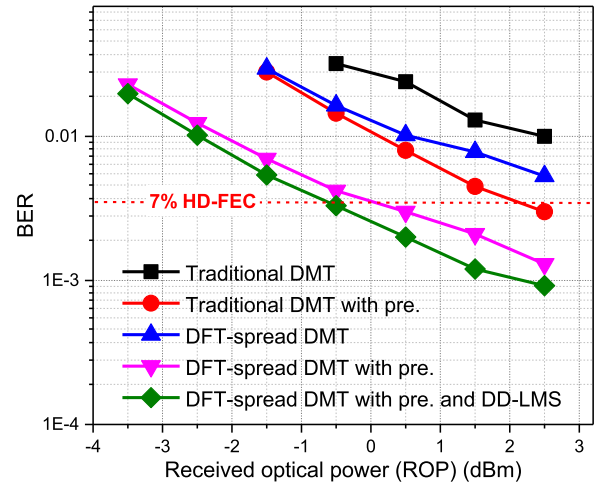
(a)



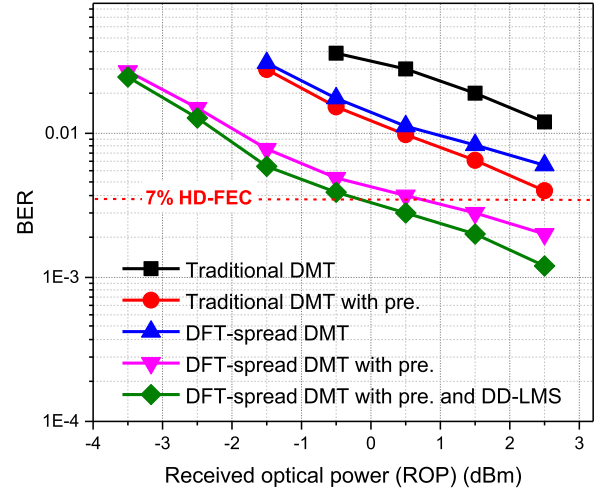
(b)

Fig. 8. BER versus ROP of 20 GHz 64QAM-DMT signal of the 2nd channel; (a) OBTB and (b) After 2.4 km SMF-28.

results are shown in Figs. 8(a) and 8(b), respectively. In OBTB, BER performance of 20 GHz 64QAM-DMT signal with pre-equalization is much better than 20 GHz traditional 64QAM-DMT signal. As DFT-spread can reduce the PAPR and overcome the high frequency attenuation to some extent, the BER performance of DFT-spread 64QAM-DMT signals is better than that of traditional 64QAM-DMT signal signals while worse than that of 64QAM-DMT signals with pre-equalization. That means insufficient bandwidth induced ISI in the established link is the main limiting factor for poor BER performance. The coordinated DFT-spread and pre-equalization technique can suppress PAPR and solve power attenuation induced serious ISI, thus 64QAM-DMT signals with coordinated DFT-spread and pre-equalization demonstrate the best BER performance. After 2.4-km SMF-28 transmission, the BER performance slightly degrades due to fiber dispersion. A BER of 3.8×10^{-3} which is the HD-FEC threshold with 7% overhead can be obtained at a ROP of -1.5 dBm and -1.2 dBm for DFT-spread 64QAM-DMT signal with pre-equalization in OBTB and after 2.4-km



(a)



(b)

Fig. 9. BER versus ROP of 20 GHz 128QAM-DMT signal of the 2nd channel; (a) OBTB and (b) After 2.4 km SMF-28.

SMF-28, respectively. A post equalizer is applied in the receiver of DFT-spread 64QAM-DMT with pre-equalization, there is 0.6 dB receiver sensitivity improvement both in OBTB and after 2.4-km SMF-28 transmission at the 7% HD-FEC threshold.

The BER versus ROP of 20 GHz 128QAM-DMT in OBTB and after 2.4-km SMF-28 transmission for the 2nd channel are also measured and shown in Figs. 9(a) and 9(b), respectively. DFT-spread 128QAM-DMT signal with pre-equalization also shows the best BER performance among four types of 128QAM-DMT signal BER performance measurement. A BER of 3.8×10^{-3} can be obtained at a ROP of 0.1 dBm and 0.5 dBm for DFT-spread 128QAM-DMT signal in OBTB and after 2.4-km SMF-28, respectively. After DD-LMS post equalizer is applied in the receiver of DFT-spread 128QAM-DMT with pre-equalization, 0.8 dB receiver sensitivity improvement is achieved both in OBTB and after 2.4-km SMF-28 transmission at 7% HD-FEC threshold. In the following test, 20 GHz DFT-spread 64QAM/128QAM-DMT signals with pre-equalization are transmitted in four channels and additional DD-LMS equal-

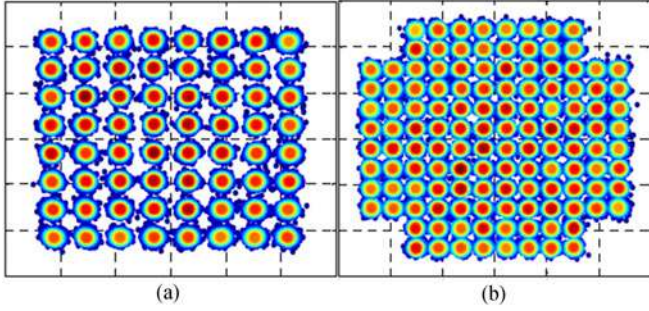


Fig. 10. Constellations of 20 GHz (a) 64QAM-DMT and (b) 128QAM-DMT.

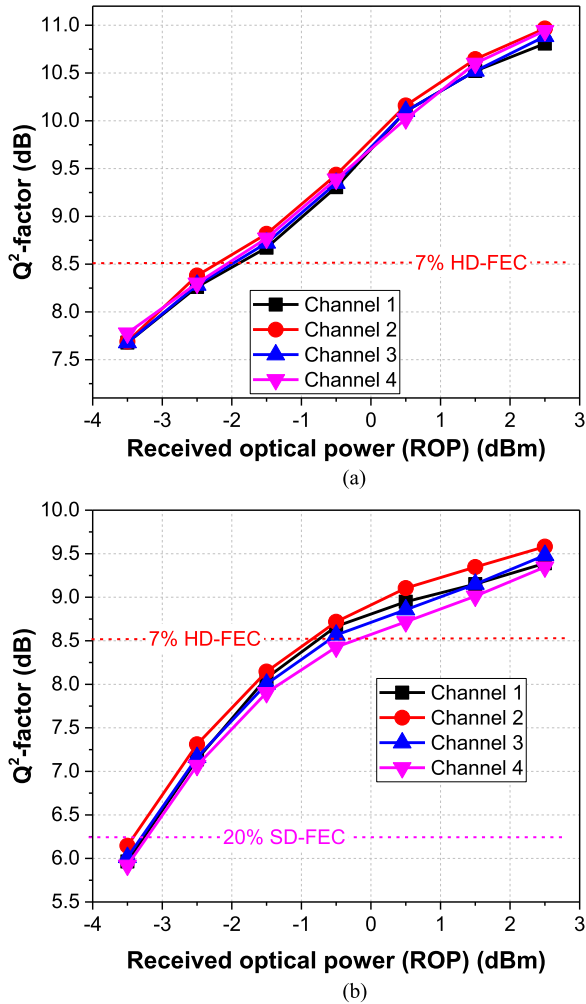


Fig. 11. BER versus ROP for four channels after 2.4 km SMF-28; (a) DFT-spread 64QAM-DMT and (b) DFT-spread 128QAM-DMT with pre-equalization and post DD-LMS equalizer.

izer will be applied in the receiver. The constellations of the 2nd channel 20 GHz 64QAM-DMT and 128QAM-DMT with coordinated DFT-spread and pre-equalization in the transmitter and post DD-LMS equalizer in the receiver at 2.5 dBm ROP are shown in Figs. 10(a) and 10(b), respectively.

Measured Q^2 -factors of four channel 20 GHz DFT-spread 64QAM-DMT and 128QAM-DMT signals with pre-

equalization and post DD-LMS equalizer versus ROP after 2.4-km transmission are shown in Figs. 11(a) and 11(b), respectively. At 7% HD-FEC Q^2 -factor limit of 8.53 dB, the required ROPs of each channel are -1.8 dBm and -0.2 dBm for 20 GHz DFT-spread 64QAM-DMT and 128QAM-DMT with pre-equalization and post DD-LMS equalizer, respectively. The total net data rate of four-channel 20 GHz 128QAM-DMT after excluding all overheads including TSs, CP and HD-FEC overhead is 513.9 Gbit/s ($560 \times 60/61 \times 8192/8206 \times 1/(1 + 7\%)$ Gbit/s ≈ 513.9 Gbit/s). To the best of our knowledge, this is a new record in 2 km short reach transmission system for high capacity interconnect. At 20% SD-FEC Q^2 -factor limit of 6.25 dB [24], the required ROPs for each channel of four-channel 20 GHz 128QAM-DMT signal transmission is -3.2 dBm with BERs. The total net data rate of four-channel 20 GHz 128QAM-DMT is 458.2 Gbit/s ($560 \times 60/61 \times 8192/8206 \times 1/(1 + 20\%)$ Gbit/s ≈ 458.2 Gbit/s) after excluding TSs, CP and SD-FEC overheads. ROP of each channel after 4-channel WDM-DEMUX is approximate 5 dBm, thus the power margin of whole link is about 8.2 dB, which indicates it is feasible to transmit 128QAM-DMT signal to realize cost-effective 2-km 400 GbE optical interconnect.

VI. CONCLUSION

We achieved the highest net data rate (513.9 Gbit/s) four-channel WDM direct detection signal transmission over 2.4-km SMF-28 with the BER under HD-FEC limitation of 3.8×10^{-3} . Both 20 GHz 64QAM-DMT and 128QAM-DMT are tested. DFT-spread and pre-equalization are jointly used to simultaneously overcome power attenuation and reduce the PAPR of the DMT signal. 0.8-dB receiver sensitivity improvement is achieved for 20 GHz 128QAM-DMT signal with the coordinated DFT-spread and pre-equalization after additional post DD-MLS equalizer is applied. The results indicate that the proposed scheme is feasible to utilize the transceiver to realize cost-effective 2-km SMF-28 link transmission to satisfy the 400 GbE standard optical interconnect.

REFERENCES

- [1] IEEE P802.3bs 400 Gb/s Ethernet Task Force. 2015–2016. [Online]. Available: <http://www.ieee802.org/3/bm/index.html>.
- [2] E. Frlan and A. Tipper, "Investigation of 50 GBd PAM-4 electrical interfaces for 2 km data center interconnects," in *Proc. Opt. Fiber Commun. Conf.*, 2015, Paper W4H.6.
- [3] J. Man, W. Chen, X. Song, and L. Zeng, "A low-cost 100 GE optical transceiver module for 2 km SMF interconnect with PAM4 modulation," in *Proc. Opt. Fiber Commun. Conf.*, 2014, Paper M2E.7.
- [4] K. P. Zhong *et al.*, "Experimental demonstration of 500 Gbit/s short reach transmission employing PAM4 signal and direct detection with 25 Gbps device," in *Proc. Opt. Fiber Commun. Conf.*, 2015, Paper Th3A.3.
- [5] L. F. Suhr, J. J. V. Olmos, B. Mao, X. Xu, G. N. Liu, and I. T. Monroy, "112-Gbit/s \times 4-lane duobinary-4-PAM for 400GBase," in *Proc. Eur. Conf. Opt. Commun.*, 2014, Paper Tu.4.3.2.
- [6] T. Chan, I. Lu, J. Chen, and W. I. Way, "400-Gb/s transmission over 10-km SSF using discrete multitone and 1.3- μ m EMLs," *IEEE Photon. Technol. Lett.*, vol. 26, no. 16, pp. 1657–1660, Aug. 2013.
- [7] T. Tanaka *et al.*, "Experimental demonstration of 448-Gbps+ DMT transmission over 30-km SMF," in *Proc. Opt. Fiber Commun. Conf.*, 2014, Paper M2I.5.

- [8] P. Dong *et al.*, "Four-channel 100-Gb/s per channel discrete multi-tone modulation using silicon photonic integrated circuits," in *Proc. Opt. Fiber Commun. Conf.*, 2015, Paper Th5B.4.
- [9] I. O. Miguel, T. Zuo, B. J. Jesper, Q. Zhong, X. Xu, and I. T. Monroy, "Towards 400GBASE 4-lane solution using direct detection of multiCAP signal in 14 GHz bandwidth per lane," in *Proc. Opt. Fiber Commun. Conf./Nat. Fiber Opt. Eng. Conf.*, 2013, Paper PDP5C.10.
- [10] T. Zuo *et al.*, "O-band 400 Gbit/s client side optical transmission link," in *Proc. Opt. Fiber Commun. Conf.*, 2014, Paper M2E.4.
- [11] W. Yan *et al.*, "100 Gb/s optical IM-DD transmission with 10G-class devices enabled by 65 GSamples/s CMOS DAC core," in *Proc. Opt. Fiber Commun. Conf./Nat. Fiber Opt. Eng. Conf.*, 2013, Paper OM3H.1.
- [12] H. Yang *et al.*, "47.4 Gb/s transmission over 100 m graded-index plastic optical fiber based on rate-adaptive discrete multitone modulation," *J. Lightw. Technol.*, vol. 28, no. 4, pp. 352–359, Feb. 2010.
- [13] K. Zhong *et al.*, "Experimental study of PAM-4, CAP-16, and DMT for 100 Gb/s short reach optical transmission systems," *Opt. Express*, vol. 23, pp. 1176–1189, 2015.
- [14] C. Xie *et al.*, "Single-VCSEL 100-Gb/s short-reach system using discrete multi-tone modulation and direct detection," in *Proc. Opt. Fiber Commun. Conf.*, 2015, Paper Tu2H.2.
- [15] P. Dong, J. Lee, K. Kim, Y. Chen, and C. Gui, "Ten-channel discrete multi-tone modulation using silicon microring modulator array," in *Proc. Opt. Fiber Commun. Conf.* 2016, Paper W4J.4.
- [16] F. Li, X. Li, L. Chen, Y. Xiao, C. Ge, and Y. Chen, "High level QAM OFDM system using DML for low-cost short reach optical communications," *IEEE Photon. Technol. Lett.*, vol. 26, no. 9, pp. 941–944, May 2014.
- [17] R. P. Giddings, E. Hugues-Salas, and J. M. Tang, "Experimental demonstration of record high 19.125 Gb/s real time end-to-end dual-band optical OFDM transmission over 25 km SMF in a simple EML-based IMDD system," *Opt. Express*, vol. 20, no. 18, pp. 20666–20679, 2012.
- [18] Z. Cao, J. Yu, W. Wang, L. Chen, and Z. Dong, "Direct-detection optical OFDM transmission system without frequency guard band," *IEEE Photon. Technol. Lett.*, vol. 22, no. 11, pp. 736–738, Jun. 2010.
- [19] Y. Gao, J. Yu, J. Xiao, Z. Cao, F. Li, and L. Chen, "Direct-detection optical OFDM transmission system with pre-emphasis technique," *J. Lightw. Technol.*, vol. 29, no. 14, pp. 2138–2145, Jul. 2011.
- [20] F. Li, X. Li, J. Yu, and L. Chen, "Optimization of training sequence for DFT-spread DMT signal in optical access network with direct detection utilizing DML," *Opt. Express*, vol. 22, pp. 22962–22967, 2014.
- [21] M. Chen, J. He, J. Tang, X. Wu, and L. Chen, "Experimental demonstration of real-time adaptively modulated DDO-OFDM systems with a high spectral efficiency up to 5.76 bit/s/Hz transmission over SMF links," *Opt. Express*, vol. 22, no. 15, pp. 17691–17699, 2014.
- [22] F. Li *et al.*, "Demonstration of four channel CWDM 560 Gbit/s 128QAM-OFDM for optical inter-connection," in *Proc. Opt. Fiber Commun. Conf.*, 2016, Paper W4J.2.
- [23] Y. Wang, X. Huang, J. Zhang, Y. Wang, and N. Chi, "Enhanced performance of visible light communication employing 512-QAM N-SC-FDE and DD-LMS," *Opt. Express*, vol. 22, pp. 15328–15334, 2014.
- [24] H.-C. Chien, Z. Jia and J. Yu, "256-Gb/s single-carrier PM-256QAM implementation using coordinated DD-LMS and CMA equalization," in *Proc. Eur. Conf. Opt. Commun.*, 2015, Paper Mo.3.3.2.
- [25] Z. Dong, X. Li, J. Yu, and N. Chi, " 6×144 Gb/s Nyquist-WDM PDM-64QAM generation and transmission on a 12-GHz WDM grid equipped with Nyquist-band pre-equalization," *J. Lightw. Technol.*, vol. 30, no. 23, pp. 3687–3692, Dec. 2012.
- [26] B. Lavigne *et al.*, "Real-time 200 Gb/s 8-QAM transmission over a 1800-km long SSMF-based system using add/drop 50 GHz-wide filters," in *Proc. Opt. Fiber Commun. Conf.*, 2016, Paper W3G.2.

Author's biography not available at the time of publication.